

# **Characterizing GEO Titan IIIC Transtage Fragmentations using Ground-based and Telescopic Measurements**

**Heather Cowardin**

*University of Texas-El Paso—Jacobs JETS Contract, NASA Johnson Space Center, Houston, TX  
77058, [heather.cowardin@nasa.gov](mailto:heather.cowardin@nasa.gov)*

**Phillip Anz-Meador**

*Jacobs, NASA Johnson Space Center, Houston, TX 77058*

**Jacqueline A. Reyes**

*University of Texas-El Paso—Jacobs JETS Contract, NASA Johnson Space Center, Houston, TX  
77058*

## **Abstract**

In a continued effort to better characterize the geosynchronous orbit (GEO) environment, NASA's Orbital Debris Program Office (ODPO) utilizes various ground-based optical assets to acquire photometric and spectral data of known debris associated with fragmentations in or near GEO. The Titan IIIC Transtage upper stage is known to have fragmented four times. Two of the four fragmentations were in GEO while the Transtage fragmented a third time in GEO transfer orbit. The fourth fragmentation occurred in low Earth orbit.

To better assess and characterize these fragmentations, the NASA ODPO acquired a Titan Transtage test and display article previously in the custody of the 309th Aerospace Maintenance and Regeneration Group (AMARG) in Tucson, Arizona. After initial inspections at AMARG demonstrated that it was of sufficient fidelity to be of interest, the test article was brought to NASA Johnson Space Center (JSC) to continue material analysis and historical documentation. The Transtage has undergone two separate spectral measurement campaigns to characterize the reflectance spectroscopy of historical aerospace materials. These data have been incorporated into the NASA Spectral Database, with the goal of using telescopic data comparisons for potential material identification. A Light Detection and Ranging (LIDAR) system scan also has been completed and a scale model has been created for use in the Optical Measurement Center (OMC) for photometric analysis of an intact Transtage, including bidirectional reflectance distribution function (BRDF) measurements.

An historical overview of the Titan IIIC Transtage, the current analysis that has been done to date, and the future work to be completed in support of characterizing the GEO and near GEO orbital debris environment will be discussed in the subsequent presentation.

## **1. INTRODUCTION**

To understand the complexities involved with the threat from orbital debris to human spaceflight and robotic missions, the NASA Orbital Debris Program Office (ODPO) is investing in different measurement and modeling techniques to acquire information on orbital debris. NASA ODPO utilizes both ground-based radars and ground-based optical assets to characterize the orbital debris population; these assets are used to better refine the data-driven environmental models used for historical, current, and future population statistics. The focus for this paper is on characterizing the limited known fragmentation events that have been observed in or near the geosynchronous orbit (GEO) regime. Specifically, of the handful of known breakups in GEO, two fragmentation events were associated with the Titan IIIC Transtage upper stage.

This paper provides a background of the Transtage, identification and characterization of a Titan Transtage test and display article, spectral measurements of various materials acquired on the test article, comparative analysis of the test article spectral measurements, focused ground-based telescopic measurements of Titan IIIC Transtage debris, and lastly, a proposed path forward to provide a more quantitative assessment of the laboratory measurements in comparison with telescopic observations that will offer insight on how and why these break-ups occur for this specific type of upper stage.

## 2. HISTORY OF TITAN IIIC TRANSTAGE

### 2.1 Physical Description

The Martin-Marietta Corporation's Transtage rocket bodies, approximately 3 m in diameter by 4.5 m long excluding specific aerospace support equipment, are comprised of a cylindrical semi-monocoque aluminum structure, consisting of a control module (forward) and a propulsion module (aft). The control module incorporates guidance, navigation, and control electronics and the attitude control system (ACS). Initially the ACS was a bipropellant system employing the same fuel (Aerozine-50)/dinitrogen tetroxide ( $N_2O_4$ ) oxidizer as the main engine, but this was later simplified to an anhydrous hydrazine ( $N_2H_4$ ) monopropellant system pressurized by gaseous nitrogen (GN2). Other stored energy sources include 28 VDC silver-zinc storage batteries and, while operational, rotating equipment in the guidance and control section. The propulsion module houses the main propulsion system, including fuel/oxidizer tanks, helium (He) pressurization systems, and the bipropellant Aerojet-General AJ10-138 dual chamber rocket engine assembly. Space-rated white paint coats the structure (Fig. 1) [1]. The asymmetric small-diameter fuel and large-diameter oxidizer tanks were exposed to the engine plume and space environment and used painted and foil insulation for thermal control the long-duration missions flown. Twin gimbaled liquid rocket engines feature blue glass frit and green painted surfaces on their nozzles as a characteristic thermal control feature.

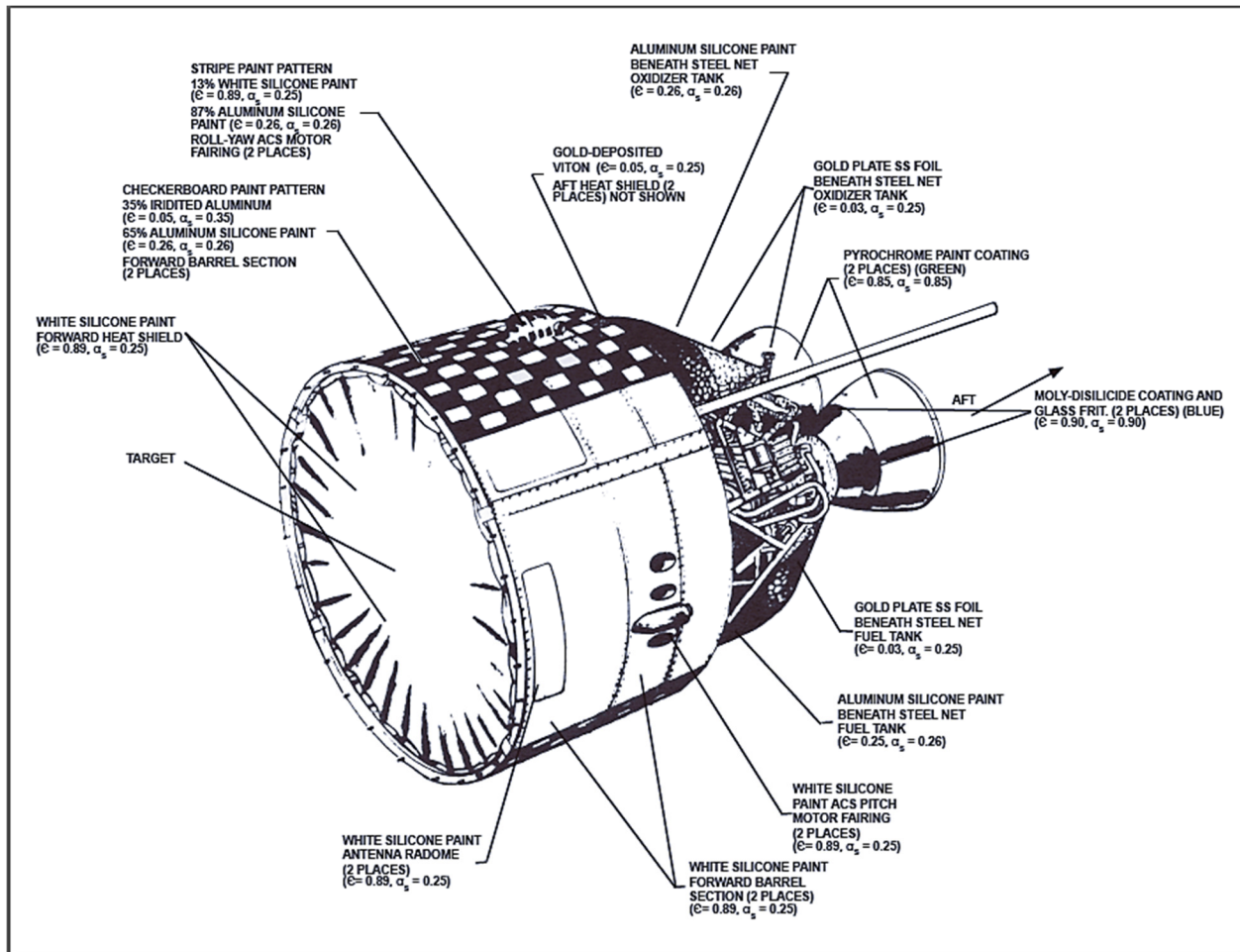


Fig. 1. Transtage thermal control surfaces and coatings of the early flight test vehicle series (vehicles 1-16).

## 2.2 Operational History

Developed in the 1960s to lift heavy payloads or multiple small payloads to specific locations in low Earth orbit (LEO) and GEO, the Transtage was the world's first "space tug" capable of multiple restarts of its engine, and could deliver multiple spacecraft to precise orbits in a single mission. Restarts were limited only by fuel and battery life. The operational history of the Transtage upper stage aboard Titan IIIA, IIIC, and 34D launch vehicles is tabulated in the Annex.

## 2.3 Known Breakups in LEO, GTO, and GEO

Two recorded breakups of Titan Transtage rocket bodies in GEO are known, as well as one in GEO transfer orbit (GTO) and one in LEO. Transtage 3C-5 (International Designator 1968-081E, U.S. Strategic Command [USSTRATCOM] Space Surveillance Network [SSN] catalog number 3432) fragmented on 21 February 1992 after 23.4 years on-orbit. Transtage 3C-17 (1969-013B, SSN #3692) fragmented on 4 June 2014 after 45.3 years on-orbit. As of 4 July 2017, the 1968-081E breakup has 28 debris pieces associated with this fragmentation but 1969-013B has no cataloged debris pieces entered into the public catalog. The GTO (1965-108A) and LEO (1965-082DM) events occurred on day of launch, likely due to propulsion-related events. The GTO and LEO events yielded 108 and 473 cataloged debris pieces, respectively; depending upon failure mode of the GEO breakups and the difficulty in cataloging highly eccentric and deep space orbits, the GEO events may have produced significantly more debris than are currently cataloged. Root causes of the GEO breakups are currently unknown, but possible causes are related to residual stored energy sources or a collision with an unknown object. Stored energy sources include batteries, unspent monopropellant and/or hypergolic propellants, and the GN2 and He pressure subsystems.

## 2.4 A Review of Suggested GEO Events

Transtage orbital perturbations have been noted by examinations of the Two Line Element (TLE) sets, and Oswald [2] asserts that these perturbations are indicative of fragmentation events. Candidates include 1966-053J, SSN #2222; 1967-066G, SSN #2868; 1973-040B, SSN #11940; 1975-118C, SSN #8516; and 1979-053C, SSN #11436.

Orbital perturbations have been regularly observed in LEO and do not in themselves provide sufficient reason to declare a fragmentation event; an exemplar is the SL-8/Cosmos-3M second stage rocket body. Many have displayed inadvertent maneuvers, in one case approximately 22 years after launch. Propellant venting has been suggested as a probable cause, and this effect may be similar to the GEO Transtage events [3]. This topic may be reexamined in light of recent analyses of GEO optical data collected from 2004-2009 and 2013-14, as well as data available from other ground-based optical assets.

# 3. NASA INSPECTION

## 3.1 Aerospace Maintenance and Regeneration Group

The authors found the Transtage test article resident at the U.S. Air Force's 309th Aerospace Maintenance and Regeneration Group (AMARG), better known as the "Boneyard," at Davis-Monthan Air Force Base in Tucson, Arizona. A June 2015 inspection by ODPO scientists Dr. Phillip Anz-Meador and Dr. Heather Cowardin determined that the Transtage object was probably an engine test article, one of the so-called "battleship" mockups used for design, integration, test, and validation, and not a flight ready vehicle. Digital images of the inspection are shown in Fig. 2 and Fig. 3.

A subset of materials was taken from the test article and analyzed at NASA JSC to compare the material's authenticity with that of the original Titan IIIC Transtage material inventory. The 28 samples were characterized via a laboratory spectrometer providing reflectance measurements in 1-nm-wide steps, from 350-2500 nm wavelengths, to identify known absorption features. The material analysis determined that the engine test article was of sufficient fidelity and a full spectral analysis in a NASA JSC environmentally controlled high bay could be used for comparative analysis with telescopic observation data of Titan IIIC Transtage fragmentation debris [4, 5]. In addition, physical

measurements could be conducted and used to create scale models for further characterization in the NASA JSC Optical Measurement Center (OMC). The specifics of the physical, spectral, and Light Detection and Ranging (LIDAR) system measurements will be discussed in Section 4.



Fig. 2. Titan III C Transtage test article stored at the “Boneyard.”



Fig. 3. Left, Dr. Cowardin acquires samples of external test article. Right, Dr. Anz-Meador acquires samples from interior of test article.

### 3.2 Transport to NASA JSC

The Titan Transtage test article arrived at NASA JSC on 26 May 2016. The following images (Fig. 4-7) show the journey of the test article from Arizona to Houston, Texas where it remains in storage. These figures help illustrate the size of the complex, asymmetric structure of this rocket body that was to be further analyzed at NASA JSC. Logistics aside, setting up the test article took coordination from various facilities, ensuring safety for all personnel, and removal of the nosecone to allow access to the interior structure to provide a more complete representative model for optical signature analysis. Once the test article was stored at NASA JSC Building 9 South (B9S), various inspections verified that it did not require any extra personal protective equipment to continue the investigation and analysis. The nose cone (or fairing) was removed to allow internal analysis of the test article, but after initial inspections found “contamination” from its long stay in the Boneyard’s desert environment, it had to be properly cleaned to remove animal/insect remains and other elements not associated with the test article. The starboard side engine bell (with respect to Fig. 2) was also removed to allow for closer inspection of the ablative materials within the thruster.



Fig. 4. The test article is lifted onto a tractor-trailer for transport to NASA JSC. (Image courtesy of Rob Raine, U.S. Air Force 309th Aerospace Maintenance and Regeneration Group).



Fig. 5. The test article arrives at JSC after a road journey shared with curious drivers. The 18-wheeler was detained going through Houston by a curious sheriff who said, “You aren’t doing anything wrong. I just wanted to see what this thing was.” (Image credit: NASA/David DeHoyos).



Fig.6. NASA JSC team members maneuver the test article into a holding cradle in theB9S high-bay. (Image credit: NASA/David DeHoyos).



Fig. 7. Nosecone removal and staging after the test article’s arrival at NASA JSC. Note sample payload attachments that show how a Titan IIIC Transtage was used to put satellites in a GEO orbit.

## 4. GENERAL CHARACTERIZATION

### 4.1 Physical Inspection of Materials and Components

Incongruous details reflect the test article’s prior history at one or more engine test facilities, the Air Force Orientation Group, and the Air Force Museum. For example, the fiberglass fairing, intended to represent the early Titan IIIA/IIIC short fairing, was installed for display purposes only, as were visible payload mockups of the DODGE spacecraft and multiple Initial Defense Communications Satellite Program (IDCSP) spacecraft. Similarly, the oxidizer tank was not authentic. In addition to the lack of an Attitude Control System (ACS), main engine pressure spheres were absent. However, general propulsion module structures, select electronics, the aft close-out/heat shield panel, the main engines and engine functional equipment, including engine bells, and the fuel tank are considered authentic original equipment. For example, the engines display considerable wear from firing, and the fuel tank is correct and displays the accurate types of insulation for this vehicle. Although the test article had been overpainted with non-space-rated aluminum

paint (structure) and yellow primer (nozzles), the ODPO collected spectral data on the underlying, original paints and coatings sufficient for future analyses (refer to Fig. 1).

#### 4.2 Spectral Measurements

The fine resolution of spectral data acquired at one phase angle can be integrated to specific bandpasses to compare with optical filter photometry for material characterization. An ASD field spectrometer with a 300-2500 nm range and a resolving power of approximately 200 (corresponding to a bandwidth of 10 nm at 2000 nm), and 717 channels was employed to acquire baseline spectral data on various material types. Because the system only needs 210 channels to obtain the desired bandwidth/spectral resolution, using 717 channels is considered over-sampling. Measurements were acquired by placing the target under a quartz lamp illuminator and orienting the spectrometer’s fiber feed (mounted in a pistol grip) approximately perpendicular to the target surface. Depending on the reflectance properties of the target/material, the angle of incidence and detector direction were modified to sample the material with maximum signal and without saturating the system.

The mean measurements were acquired when there were enough samples to compute an average spectrum; therefore, the data presented will use a “.mn” extension in all legends to demonstrate when a mean sample was utilized. One exception is “blueglassfritR3.sco,” whose single measurement showed enough interesting features to include even if it was statistically insignificant and did not show a repeatable sequence of measurements. The data were output to a laptop computer and reduced using in-house developed software to provide the absolute spectral reflectance. In order to provide a calibrated reflectance, a Spectralon panel is utilized to provide an absolute reflectance measurements. The processed data will be uploaded to the JSC Spacecraft Materials Spectral Database. Analysis of three different data collects was conducted to compare the spectral measurements acquired from the test article. The first data collect was based on the 28 samples removed in Arizona. The second data collect was conducted at NASA JSC after the test article was deemed safe for continued analysis. The last data set was a repeat of the same materials analyzed during the second data collect, but each material was cleaned with water or isopropyl alcohol to remove dust/debris/oxidation and compare how the spectral measurement reflectance properties changed.

The following plots show the spectral measurements acquired during the three data collects and discussion follows on the commensurate 12 materials (see Table 1) deemed appropriate and of greatest significance for comparison. Nomenclature for the curves on each plot are designated with a preceding title of either “Sample\_”, “9S\_”, or “9SClean\_”, for differentiation between data collects on samples retrieved from AMARG in Arizona, the test article surface as received at NASA JSC in B9S, and the surface after cleaning at NASA JSC, respectively.

Table 1. List of materials used for comparative analysis taken from the multiple data collects of the test article.

001	Blue Glass Frit
002	Dark Checkerboard Locations
003	White Checkerboard Locations
004	Columbium Metal
005	Engine Shroud
006	Exposed Engine Bell
007	Exposed Metal Top
008	Gold Foil
009	Green Paint
010	Red Paint
011	Strut
012	White Paint

The first set of analyzed spectral data to be presented focuses on blue glass frit located on the test article’s engine bell, shown in Fig. 8. Spectral readings obtained from the test article’s glass frit surfaces were all acquired after transport to NASA JSC’s B9S. The data acquired during the initial measurement campaign exhibit greater evidence of blue

color absorption features than their cleaned counterparts did. The data labeled “blueglassfritR2.sco” is the only spectra data that was taken where a mean statistic was unable to be acquired. This single measurement shows a deep (wide) absorption feature starting near 300 nm and ending close to 750 nm. Reflectance curves exhibit relatively flat spectral curves past the visible region (~800 nm), best correlated to the presence of metallic elements within the composition, due to a moly-disilicide coating integrated with the glass frit on the test article. No indication of organic presence resulted from the two data collects involved with glass frit materials taken in B9S.

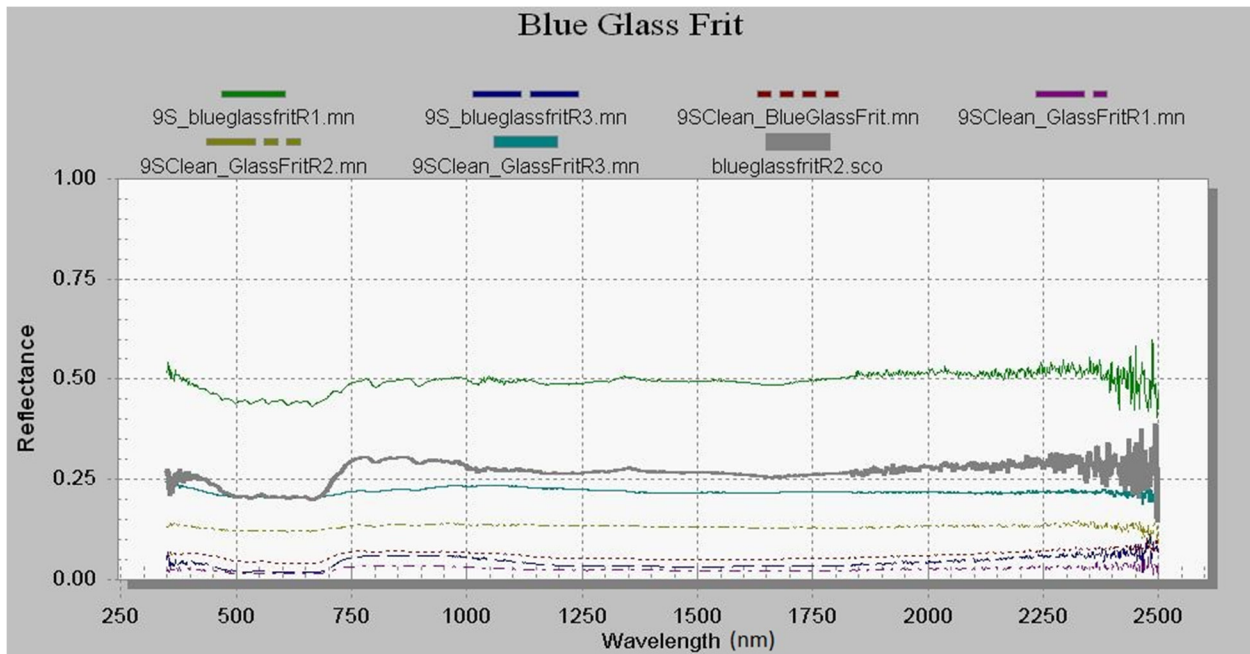


Fig. 8. Reflectance spectra of blue glass frit specimens superimposed with similar glass frit materials taken from unclean and clean test article surfaces. The data labeled “blueglassfritR2.sco” belongs to an unclean surface spectral reading.

The next set of spectral measurements targeted the unique checkerboard pattern on the test article’s barrel section (refer to Fig. 1). Although the schematic shows 35% iridited aluminum and 63% aluminum silicon paint, the exact material used for the “dark” and “light” checkerboard regions are not well known. Future work may include using inductive coupled plasma mass spectrometry analysis (ICP-MS) to verify the actual composition of checkerboard patterns. The darker checkerboard regions on the test article exhibit a slight aluminum feature at 850 nm common between all three data collects, referred to as “Dark Checkerboard” (Fig. 9). The silver paint checkerboard sample, “Sample\_SlvrPaintChkrbrd.mn” retrieved from AMARG, demonstrates prominent organic features at 1500 nm and ~1930 nm wavelengths that could be due to water (H<sub>2</sub>O) and carbon-hydrogen (C-H) bonds often present in organic material. Counterparts to its dark regions, the test article’s light checkerboard regions, referred to as “Light Checkerboard,” are shown in Fig. 10. The data acquired on the white paint checkerboard sample recovered from the AMARG initial inspection titled “Sample\_WhitePaintChkrbrd.mn” exhibits slight organic features, similar to the dark checkerboard sample titled “Sample\_SlvrPaintChkrbrd.mn” shown in Fig. 9.

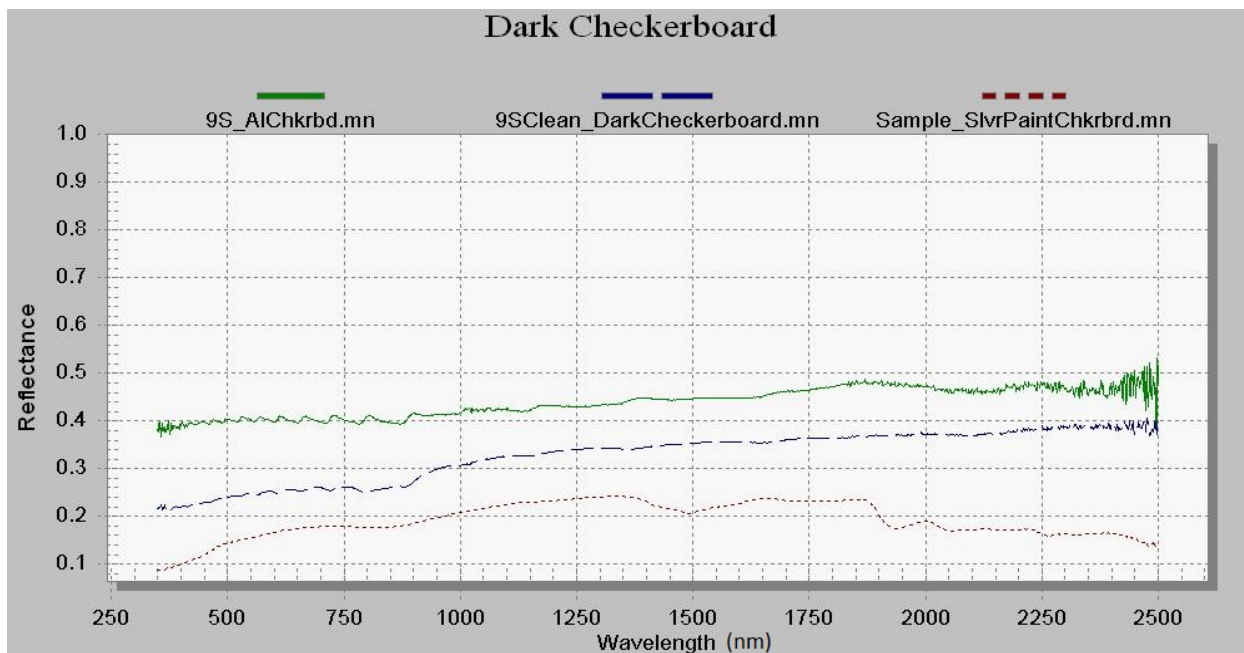


Fig. 9. Reflectance spectra for dark regions located on checkerboard pattern on test article’s exterior.

The checkerboard barrel section samples of the test article retrieved from AMARG, both dark and light checkerboard regions, were removed through the use of standard sandpaper. The analysts did remove the bias from the sandpaper spectra response; however, organic features existing on the retrieved samples’ curves could be a result of contamination from the sandpaper utilized, whereas these organic results are unseen on spectra obtained from the clean and unclean test article (Fig. 9 and Fig. 10). Therefore, surfaces on the test article in both the “as received” and cleaned conditions display aluminum features while showing no indication of organics present for their respective spectra.

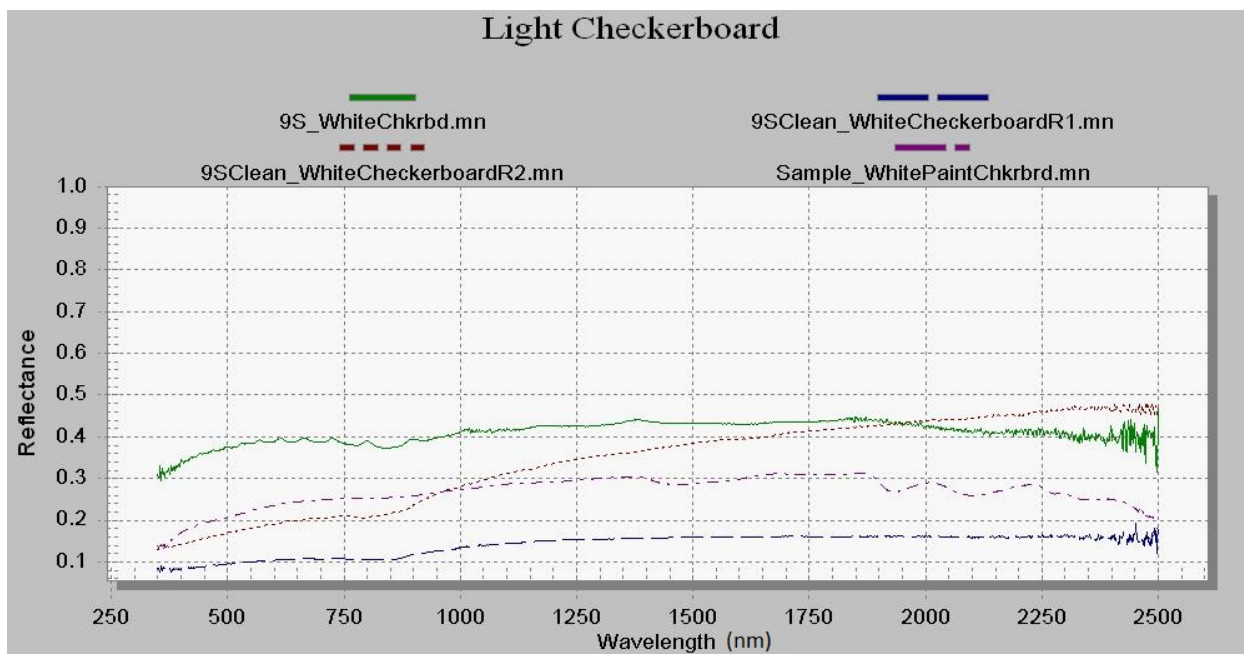


Fig. 10. Reflectance spectra for light regions located on checkerboard pattern on test article’s exterior.

Fig. 11 represents spectra taken from the test article's engine bells with focus on the exposed Columbium (Cb) that would be underlying the blue glass frit. No samples could be removed during the AMARG visit, thus data presented will be only for measurements acquired post-transport to NASA JSC. The spectra in Fig. 11 are representative of metallic materials (non-organic), noting the increase in slope into the short wave infrared wavelengths (> 1100 nm). The uncleaned and cleaned test article surface data sets are consistent with each other, presenting curves low in reflectance (<10% or 0.1) with a continuous increase in slope (near 20% or 0.2). The absence of any organic or aluminum absorption features in the obtained spectra is consistent with our knowledge of Cb. A literature review into reflectance properties for pure Cb, also known as Niobium (Nb), showed an evident absorption feature present at approximately 350 nm with an increasing slope, as noted in the test article spectral data [6]. The lack of this feature near 350 nm is presumably because the material used for the test article was C103 Cb alloy [7, 8]. Similar to the above-mentioned checkerboard pattern materials, future work may include using ICP-MS to verify the true composition of the Cb alloy.

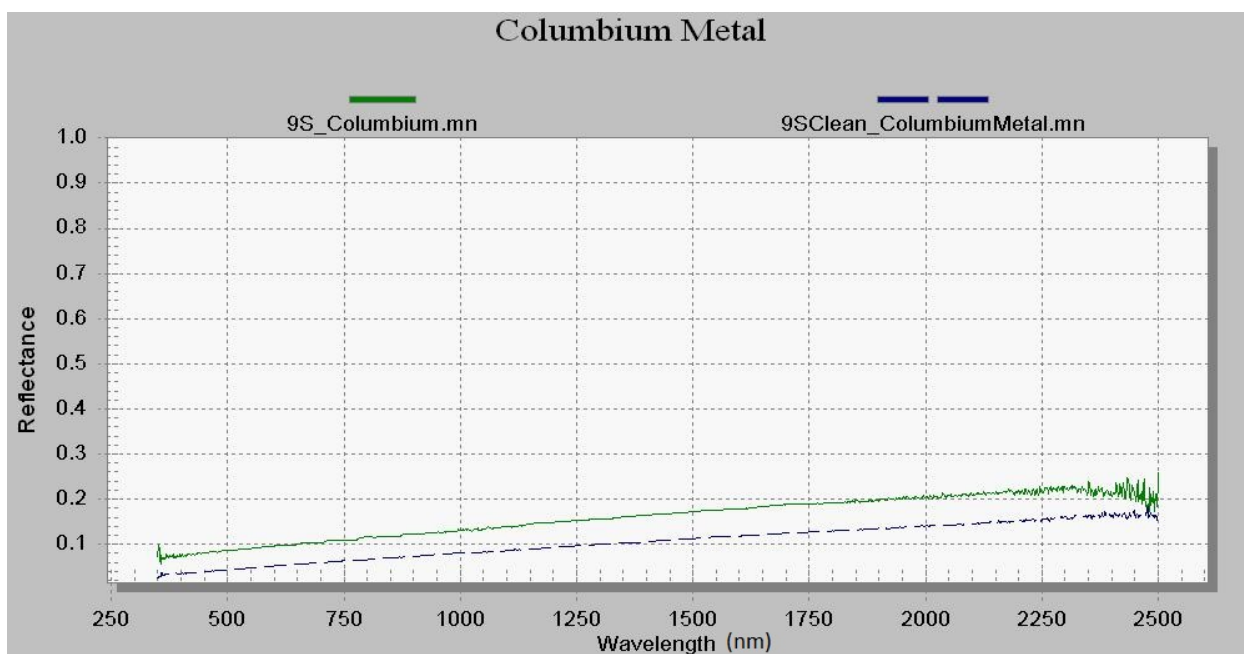


Fig. 11. Reflectance spectra taken on “as received” and clean surfaces of Cb-related metal on the test article in B9S.

Spectra taken on the various materials shown in Fig. 12 are in reference to the test article's engine shroud. This test article material was not cleaned during the post-cleaning campaign because of its fragile state after exposure to harsh environments during storage at AMARG. The fiber matting cloth sample from AMARG and the uncleaned test article close out panel/thermal shield readings demonstrate curves most comparable to one another; however, all three spectra data collects show a presence of organic elements within these materials. The absorption features near 1400 and 1900 nm indicates an H<sub>2</sub>O feature and the absorption features centered at 2100 and 2300 nm indicate a C-H bond. The wide bandgap at 1500 nm likely is due to the close out/shield cloth material.

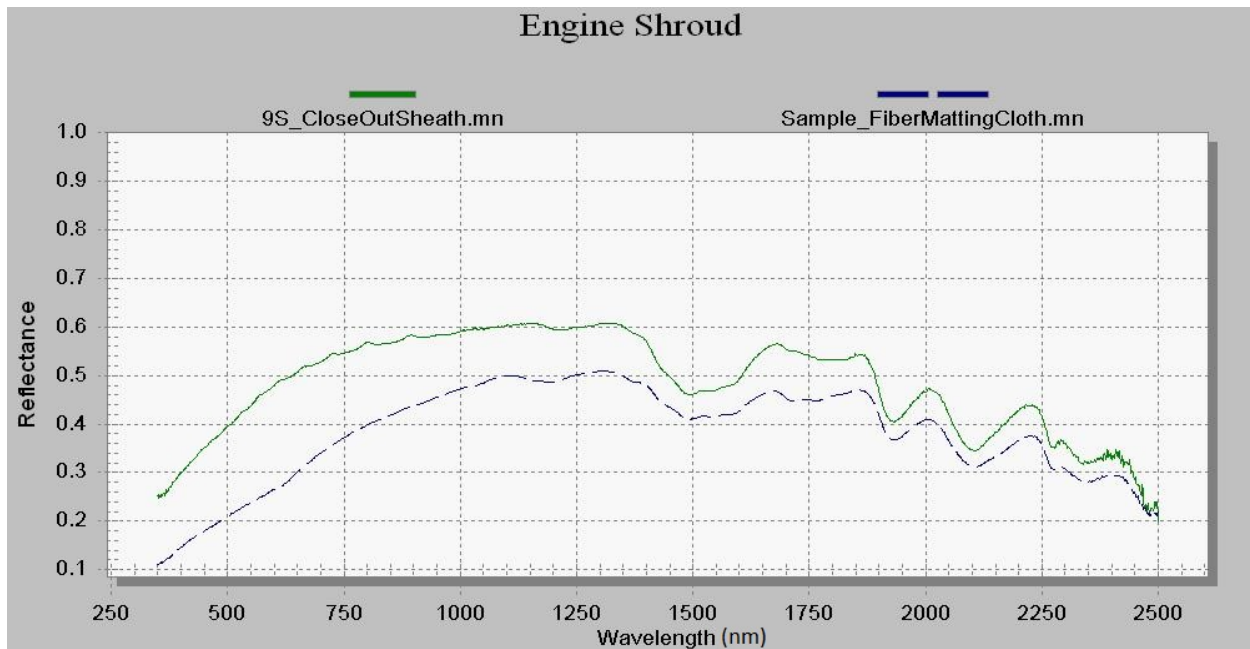


Fig. 12. Reflectance spectra of engine shroud found aft of the test article barrel section.

Spectral readings obtained on the unclean and cleaned exposed engine bell surfaces of the test article, shown in Fig. 13, indicate color absorption features (perhaps due to green paint and the yellow, non-flight primer paint) that were used on the aft extension of the engine bell. Also noted is the lack of an aluminum feature and a flat reflectivity response from 750 -2500 nm indicative of a metal, probably titanium. The exact composition of this material can be analyzed with further research as mentioned previously with the checkerboard pattern surface materials and Cb.

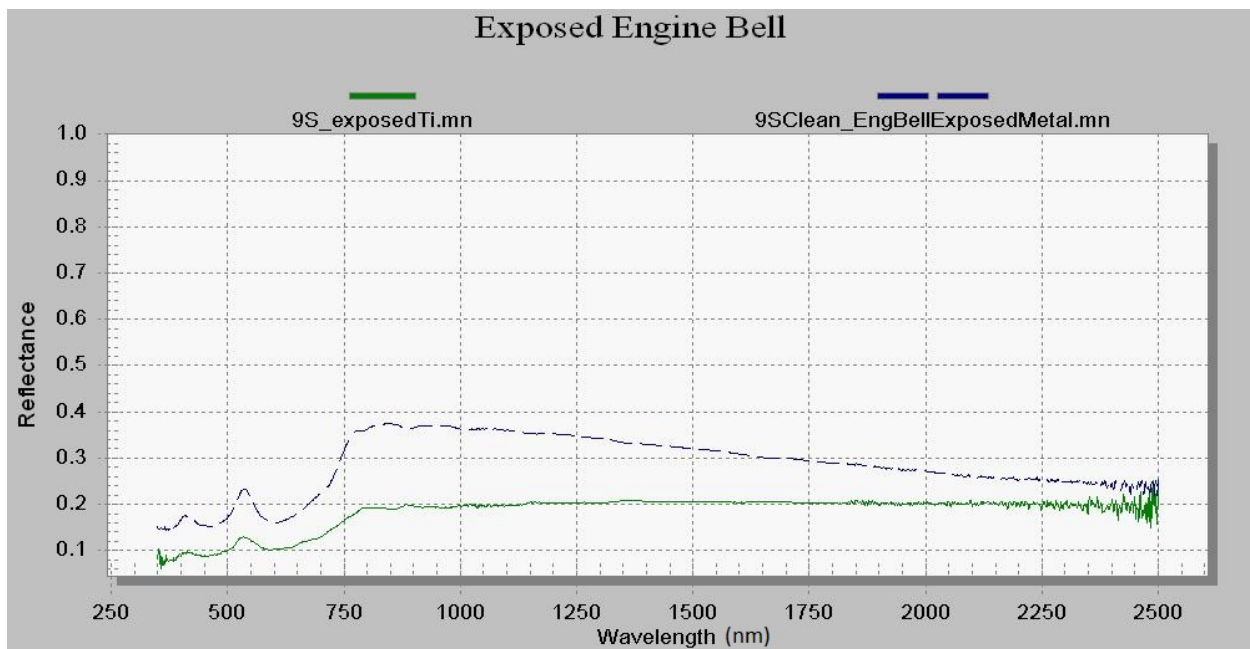


Fig. 13. Reflectance spectra corresponding to exposed engine bell on the test article in B9S.  
No sample data acquired.

In Fig. 14, reflectance spectra from the test article’s exposed metal on the top of the barrel (as seen from the ground in B9S) were only collected post-transport to NASA JSC, but the prior data collects taken during the pre-clean measurement campaign at NASA JSC offered insufficient results for a comparison standpoint. Although reflectance varies between the spectral data analysis for the bare metal top, it can be determined that the material mainly consists of aluminum with common occurrences in absorption at 850 nm.

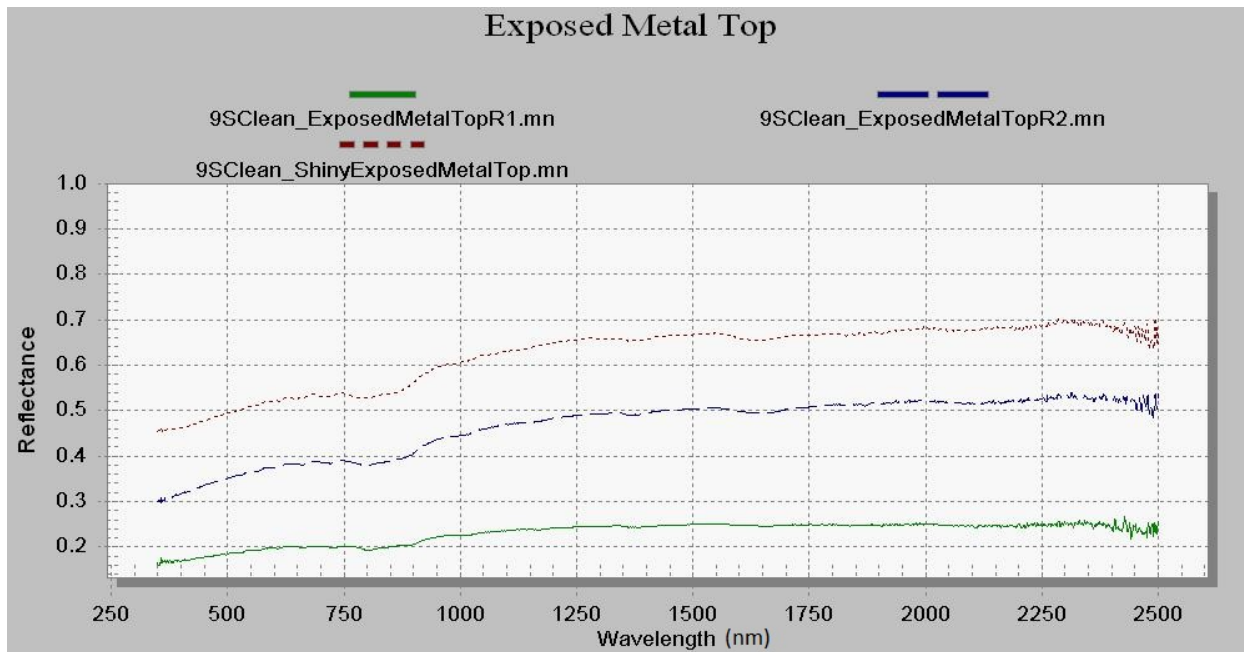


Fig. 14. Reflectance spectra taken from cleaned test article in B9S for material characterization of bare barrel surface.

Similar to the circumstances with the engine shroud material, measurements and analysis of the gold foil located on the test article’s oxidizer tank were conducted only on the samples retrieved from AMARG; however, it still has features of interest to evaluate. In Fig. 15, the spectra plot depicts a clearly evident gold/yellow color band gap between 350-600 nm with minor organic traits present at 1150 nm and 1950 nm wavelengths. Often, foil is composed of aluminum coated in oxides to enhance corrosion resistance [9]. If the test article’s gold foil has these typical properties, then it can be inferred that this is responsible for the organic spectral results. The spectrum pertaining to the gold foil reaches above 100% reflectance, suggesting that the laboratory instrument was saturating due to its inability to accept such increased specular reflections.

Spectral readings acquired from all three data collects involving green paint on the engine bell of the test article demonstrate prominent green color band gap traits in existence at approximately 500 nm (Fig. 16) and slight organic features revealed in all materials, excluding the green paint taken from the cleaned surface designated as “9SClean\_GreenPaintEngineBell.mn.” The green paint overlays the engine bell as a coating, raising the possibility that the cleaning removed some paint oxidation remnant, thus minimizing the organic features from the engine bell’s spectrum and making it inconsistent with previous spectral results.

The spectral measurements acquired on the red-pigmented paint located at various locations (internal and external) on the test article were examined, as shown in Fig. 17. The red colored paint bandgap is present near 550-600 nm for all material readings, with the right primer sample, “Sample\_RightPrimer.mn,” recovered from the test article at AMARG showing the highest reflectivity (>50%) in comparison to all other red paint measurements. Again, the right primer sample is unlike its associates due to its exhibition of aluminum presence with an absorption occurrence at 850 nm. The measurements acquired on the red paint from the exterior surfaces suggest the same primer probably was not used for the exterior and interior surfaces of the test article.

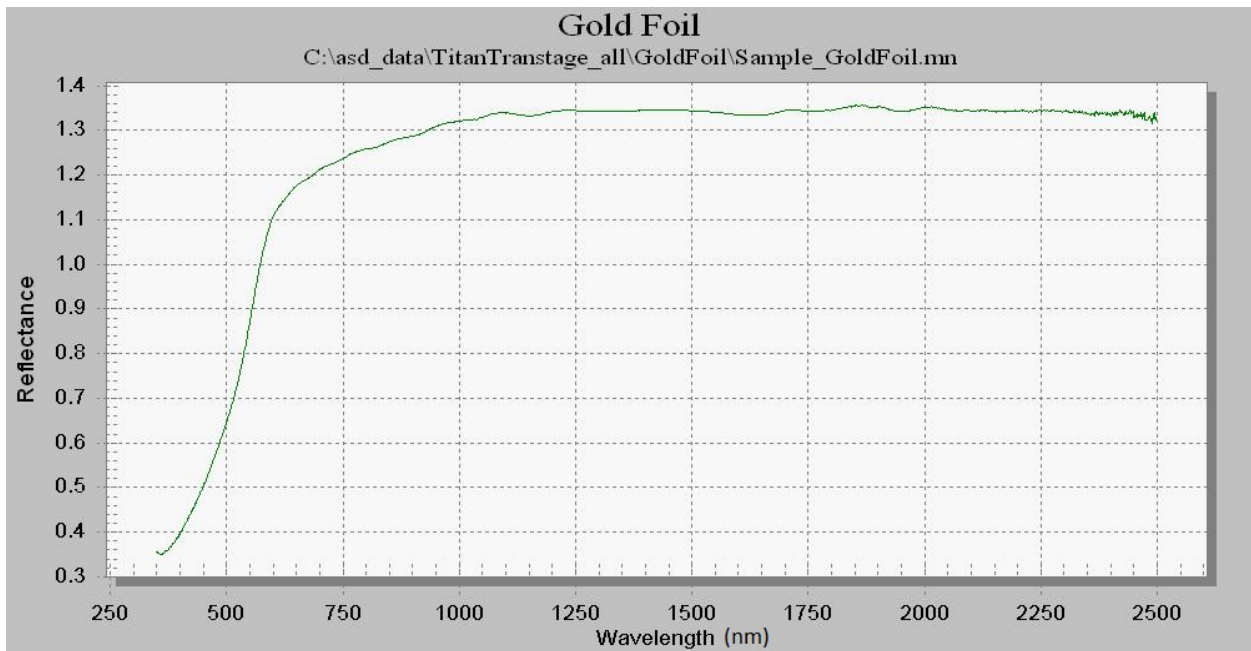


Fig. 15. Reflectance spectrum for gold foil samples taken from the test article at AMARG.

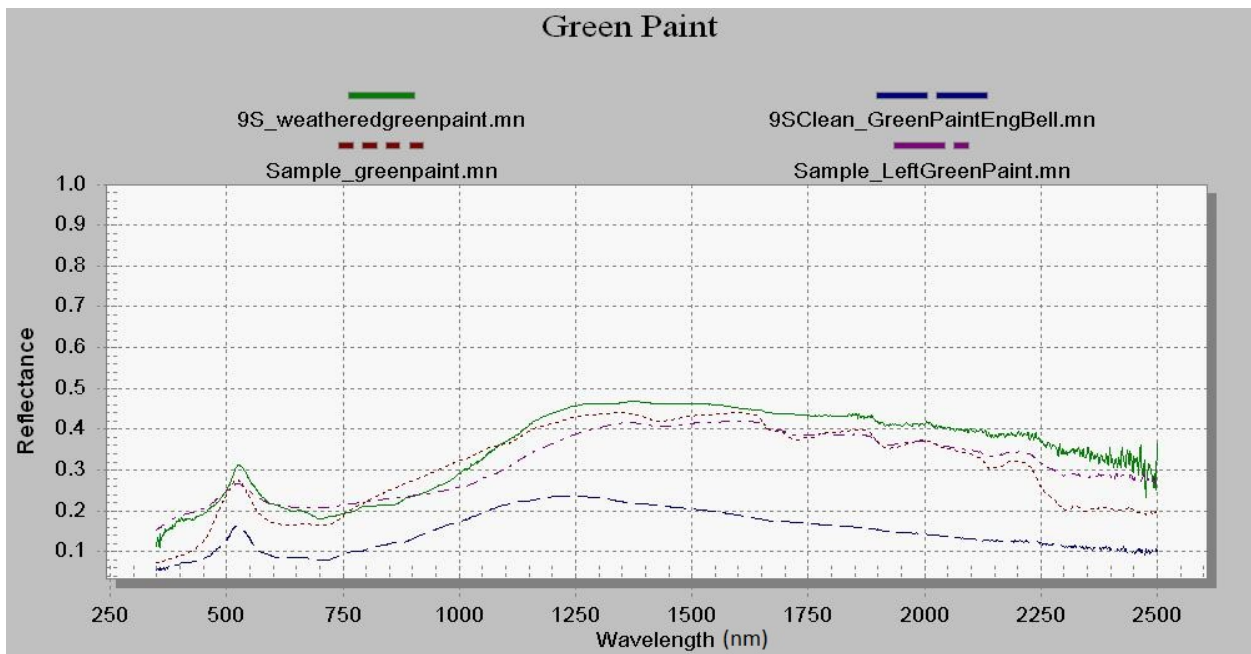


Fig. 16. Reflectance spectra for various green paint regions present on the test article's exterior engine bell.

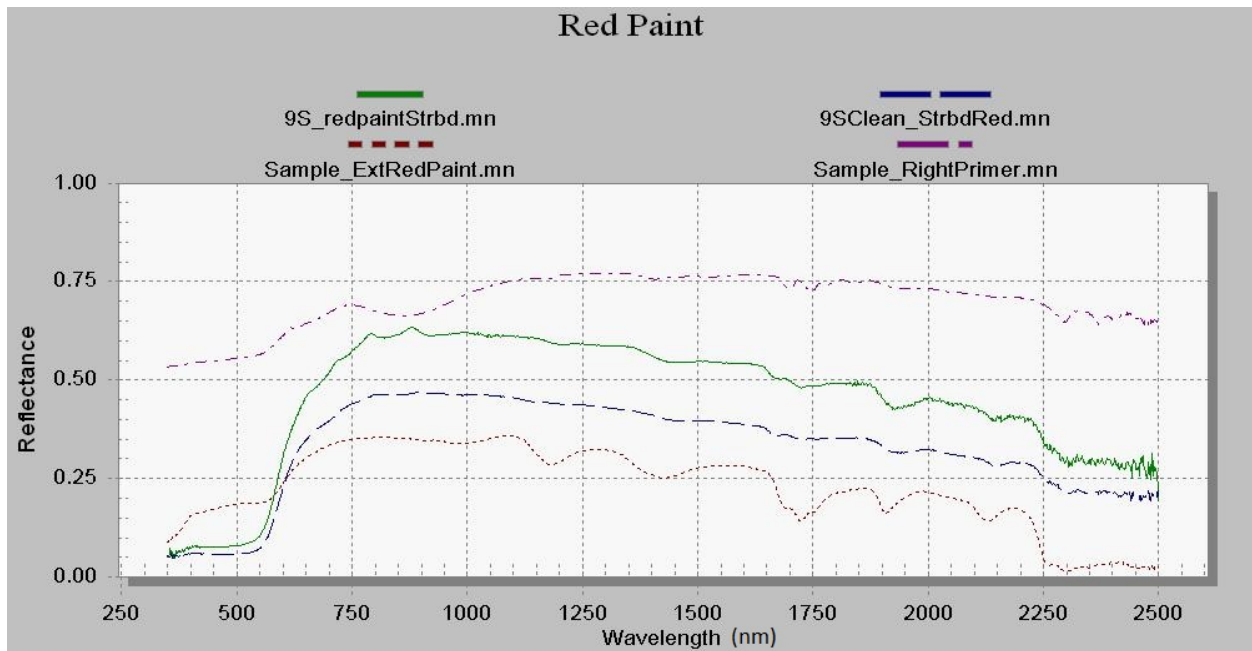


Fig. 17. Reflectance spectra for red paint on various exterior regions of the test article.

Reflectance spectra data taken on the struts, located at the aft of the test article’s barrel within the fuel tank and engine bell volume, were only done post-transport to NASA JSC; thus, the cleaned and uncleaned surfaces are presented in (Fig. 18). The spectra data acquired from all measurements shows the presence of aluminum near 850 nm. The feature near 1650 nm is similar to absorption features found on spacecraft metals that use a specific coating for the harsh environment of space.

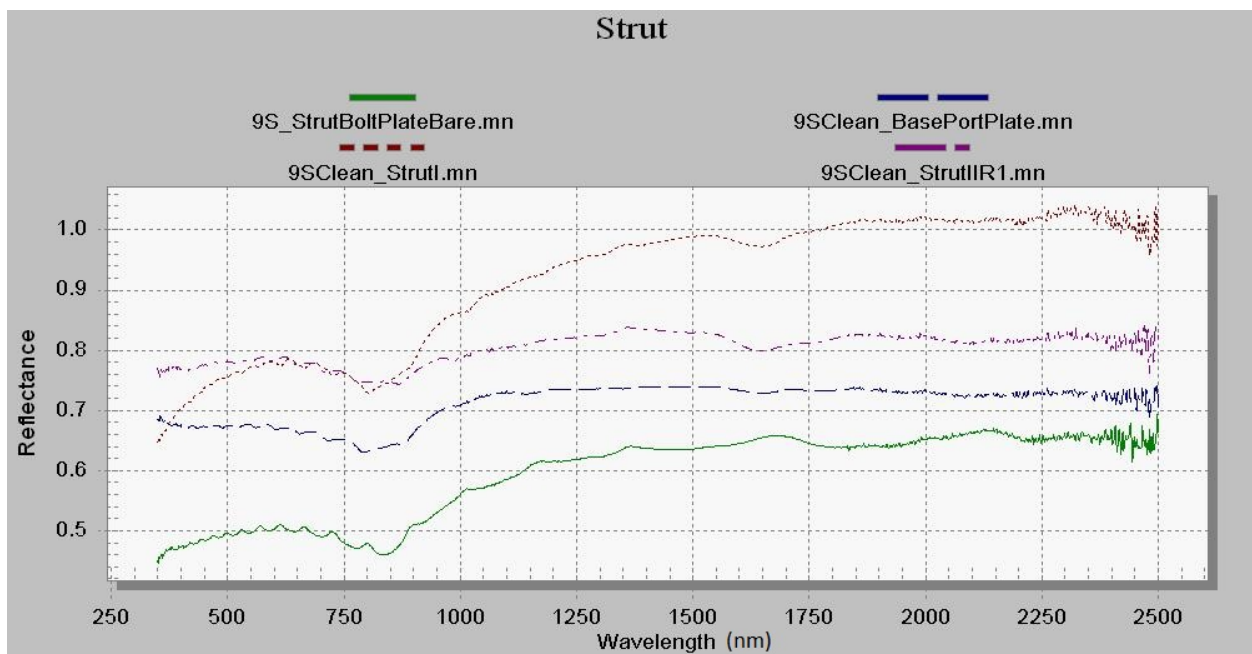


Fig. 18. Reflectance spectra taken on “as received” and clean surfaces of the test article in B9S.

In Fig.19 spectral data of white paint found on the exterior of the test article is shown. The consistency between the multiple white paint spectral readings is sufficient, presenting apparent white band gaps at approximately 400 nm followed by organic features beyond 1100 nm, most likely due to the test article’s respective paint properties. The white paint sample, “Sample\_OrigWhtPaint.mn,” showed equal reflectivity measurements as that of the “9S\_WhitePaintPort.mn” data. The cleaning process significantly increased the reflectance properties for the “9SClean\_PortWhitePaint.mn” sample, although minimal effects were seen with the white paint samples taken from the starboard side. Paints often utilize H<sub>2</sub>O as a solvent, and O-H-C-H bonds are found in paint binders, which are used to secure pigment and therefore take on polymeric properties [10]. These molecular bonds, or any additional organics discovered within their respective paint compositions, presumably could be responsible for the absorption features beyond 1000 nm for blue, green, red, and white paints. These, as discussed previously, were examined for further material characterization of the test article. Preliminary analysis indicated the paint sampled from the port and starboard sides was not consistent, and the sample acquired from AMARG is consistent with the starboard side of the test article.

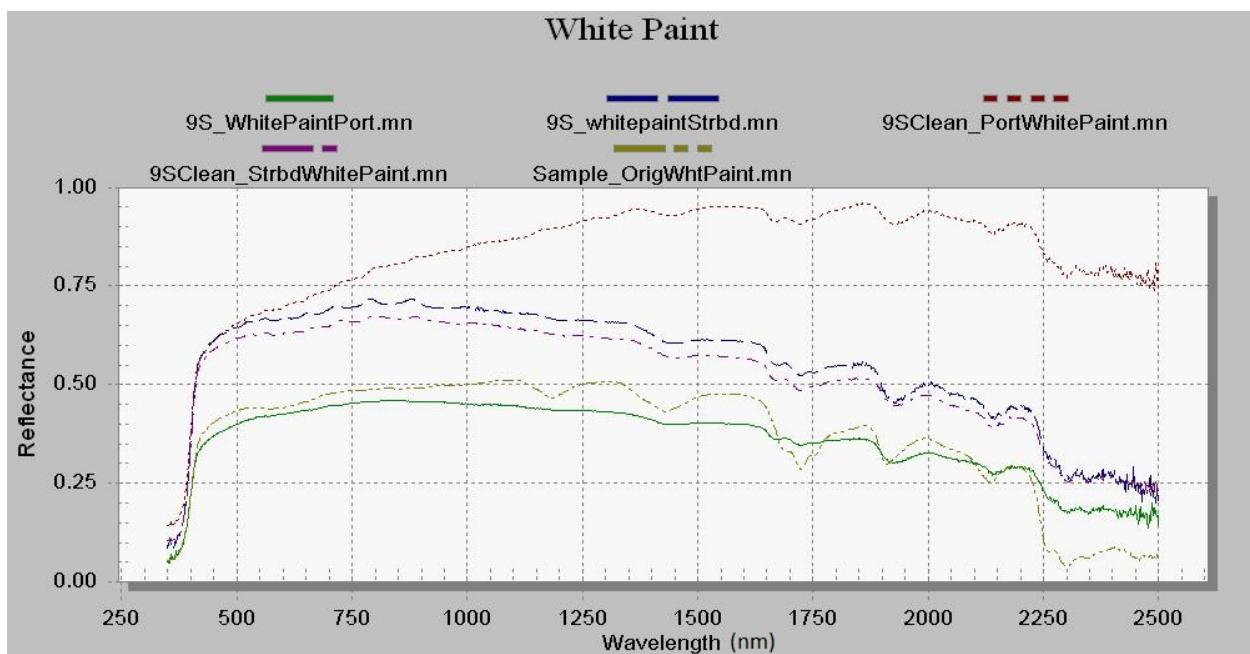


Fig.19. Reflectance spectra corresponding to various regions of white paint present on surfaces of the test article.

### 4.3 LIDAR Measurements

To better characterize the test article for future research, a scale model will be made in a size that will be used for OMC lightcurve signature analysis. A secondary goal is to generate a 3-D point cloud from a scan of the entire test article and then use software codes to test theoretical explosion/fragmentation events based on hydrocode analysis of known targets. To meet these requirements, the Image Science and Analysis Group (ISAG) at NASA JSC provided support via a handheld LIDAR system mounted on an iPad Air 2 [11, 12]. Because the test article was much larger than the LIDAR’s intended use, the team collected approximately 60 scans and images, which they ordered topologically to ensure completeness in the scanning collection. The instrumentation created a 3-D point cloud with a digital overlay as shown in Fig. 20 and Fig. 21.



Fig. 20. LIDAR digital overlay of the test article.



Fig. 21. LIDAR digital overlay, payload end (left), thruster end (right).

## 5. TELESCOPIC OBSERVATIONS FOCUSED ON TITAN IIIC TRANSTAGE FRAGMENTS

The Titan IIIC-5 Transtage (1968-081E) fragmentation pieces were observed over numerous data campaigns using Johnson/Bessell filter photometry with the Michigan Orbital Debris Survey Telescope (MODEST) 0.61-m Curtis Schmidt telescope and the Cerro Tololo Inter-American Observatory (CTIO) 0.9-m telescope, and a visible regime spectrograph with the 6.5-m Clay Magellan telescope at the Las Campanas Observatory. Photometry data were compared with previously collected laboratory photometry data (International Designator 1968-081, SSN numbers 3432, 25001, 33509, and 33510) to correlate materials. Spectral data were compared with laboratory spectral data on known materials associated with the Titan Transtage (International Designator 1968-081E, SSN #25000 acquired over two observing periods – May 2012 and January 2013, and SSN numbers 38690 and 38699) based on shape characteristics and slope factors [13]. Limited results of the investigation are shown in Table 2. Note the titan article was not available for previous research analysis, thus the correlations presented are based on sample fragments from previous fragmentation experiments or spacecraft material samples.

Future work will include a thorough investigation of the past-observed data with the most recent spectral data taken from the test article at NASA JSC. The material associations are based on color-color plots and absorption features for the photometric and spectral data, respectively. The preliminary correlation between laboratory and telescopic data does provide insight into the primary surface material observed from the break-up events associated with 1968-081E. The larger fragment (SSN #3432) matched with a 1960s era Transit satellite composite material sample from previous laboratory studies, suggesting that it is a mixture of various materials including white paint, metal, and dielectrics, as shown in Fig.22. The other correlated laboratory pieces matched that of white paint and aluminum, as found on multiple surface structures of the Titan III Transtage. SSN #38690 showed aluminum features, but with black paint (or possibly darkening due to an explosive event) and particulates, when compared with laboratory breakup

samples from previous experiments. The last fragment that showed a close correlation to blue/green paint is consistent with the Titan IIC Transtage engine bells, see Fig. 1.



Fig.22. Composite fragment from an impact experiment based on a 1960s era Transit satellite. The color-color plot matched the closest with the observed SSN 3432 Titan Transtage fragment.

Table 2. SSN observed fragments and most feasible material association based on laboratory analysis

SSN	Material	Likely Candidate Materials
3432	Dielectric	composite
25000	Dielectric	white paint
25001	Dielectric	composite/electronic circuit board
33509	Metal	aluminum
33510	Metal	aluminum
38690	Dielectric/Metal	black paint/aluminum covered with particulates
38699	Dielectric	blue/green paint

The United Kingdom Infrared Telescope (UKIRT) was also used to collect spectral measurements of fragmentation debris associated with the Titan IIC Transtage breakups. A subset of spectral data on focused targets, generally the fragments with the larger radar cross sections, is presented below. International Designator 1969-013B, SSN #3692 is a rocket body from a Titan IIC Transtage 2014 fragmentation event; see Fig. 23 [14]. International Designator 1976-023J, SSN #8832 is mission-related debris, an apparently intact object (not fragmented debris) associated with the deployment of the mission’s payload in GEO, shown in Fig. 24 [14]. The increase in slope shown in both spectral plots is consistent with silicon features found in spacecraft paints and silicon-based solar cells; noting that because no solar cells are associated with the Titan Transtage IIC target, the most likely correlation is paint. A more diverse collection of ground-based measurements, including visible and infrared, with multiple observations of the same target would be required to provide better insight into the surface material(s) observed in respect to Titan Transtage fragments and associated debris (rocket bodies and mission related).

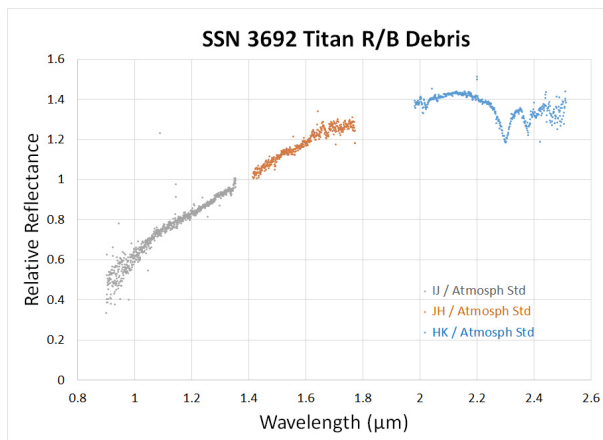


Fig. 23. UKIRT spectra of SSN 3692

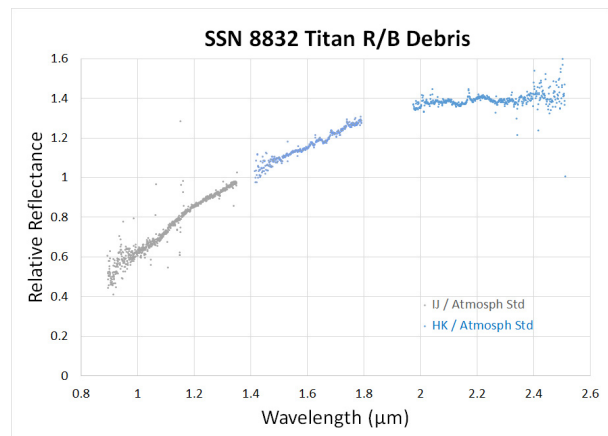


Fig. 24. UKIRT spectra of SSN 8832

## 6. PLANS FORWARD AND CONCLUSION

This paper has described activities related to the goals of:

- (1) Assessing the intact state of the Transtage on-orbit population, excepting those vehicles known to have fragmented;
- (2) Inventorying the stored energy reservoirs aboard the Transtage vehicle;
- (3) Inventorying the aerospace materials aboard the Transtage vehicle; and
- (4) Defining a meaningful rubric which could be used by ground-based filtered-photometry telescopic sensors to assess the materials found in debris and thereby associated given Transtage debris with a component, system, or subsystem of the Transtage vehicle. This may enable the causality of fragmentations to be established and inform environmental modeling and surveillance of this vehicle population.

The first goal has been addressed in our inspection of the Transtage test article, including the LIDAR characterization of the surface. The LIDAR data presented in this document is only part of Phase I of this project. Phase II will include removing artifacts (such as the damaged side of the barrel shown in Fig. 20 and Fig. 21), as well as incorporating modeled components of the Titan Transtage that were not found on the test article. The LIDAR data from Phase II will be used to create 3-D printed articles for analysis at the NASA JSC OMC. The scaled Titan IIIC Transtage will be mounted on a 6-degree-of-freedom robotic arm to characterize the reflective properties from an intact Transtage using bidirectional reflectance distribution measurements. Using the OMC measurements and analysis of an intact Transtage can provide insight into observed optical lightcurves and properties-specifically determining the uniqueness of the optical signatures of intact and fragmented Transtage vehicles. Also associated with this task is an anticipated survey of historical orbital data, the TLEs, to better understand the orbital evolution of the Transtage population, including any impulsive events noted.

The second goal has also been addressed by our inspection of the Transtage test article and associated background engineering literature review.

The third goal is addressed by using the spectral data and the LIDAR data to assist in laboratory characterization of a Titan IIIC Transtage test article and will provide more insight into the materials associated with the break-up events, potential causes of fragmentation events for this specific target, and materials-dependent risk associated with these Transtage break-ups observed in various orbital regimes.

Future plans for this project, essentially associated with our fourth stated goal, include further analysis of the spectral data collected, quantifying the uniqueness of the materials associated with the test article/Titan IIIC Transtage, and providing a material taxonomy using all the materials in the NASA spectral database. ICP-MS analysis also will be used to resolve the exact composition of various materials noted in the spectral analysis of the test article. The spectra data can be integrated into broadband astrometric filters, as was done in Ref. 13, to further analyze telescopic and laboratory correlations. The spectra acquired from the test article that have been defined as authentic and adequate for comparison to original materials also can be used to provide a better, more thorough database for spectral un-mixing in regard to disintegrating the spectral response acquired from ground-based telescopic data. The goals are to better understand the observed fragments from various telescope assets to support characterization of the GEO orbital debris environment. To date, the data observed has only been used for statistical interpretation in a GEO survey mode. Future work will investigate material associations of the fragments to the Transtage to better define density and likely shapes associated with these fragmentation events.

This paper highlights the current data that has been acquired in order to characterize fragmentation events associated with the Titan IIIC Transtage. Future work has been outlined that will support environmental models and insight into how intact Titan upper stage rocket bodies are fragmenting, specifically investigating the completeness and uniqueness of material characterization to determine the source of Transtage debris (and debris of unknown origin) and provide insight via optical signature analysis to determine if the fragmentation is due to stored energy explosion, collision with untracked object, or other failure modes that should be investigated.

## 7. ACKNOWLEDGEMENTS

The authors would like to acknowledge the following colleagues who were crucial to moving the test article to NASA JSC and for their contributions to the on-going work associated with this paper. Special thanks to Lisa Pace (NASA) for initiating and leading the transport paperwork and our JACOBS-JETS logistics team, led by Donna Castillo. Thanks to the ISAG at NASA JSC, specifically, Mr. Joseph Aebersold, for acquiring the LIDAR measurements presented in this paper.

## 8. REFERENCES

1. Sousek, D.D., "Orbital Simulation of the Titan III Transtage Spacecraft." Proc. IES **12**, 561-76, 1966.
2. Oswald, M., New Contributions to Space Debris Environment Modeling. Shaker Verlag, 2008.
3. Johnson, N.L., "Evidence for Historical Satellite Fragmentations in and near the Geosynchronous Regime." In Proc. Third European Conf. Space Debris ESA SP-473, 355-9, October 2011.
4. "Titan Transtage Arrives at JSC to be Studied by Orbital Debris Scientists," Orbital Debris Quarterly News Vol 20, Issue 3, July 2016.
5. <https://sma.nasa.gov/news/articles/newsitem/2016/06/07/orbital-debris-program-office-to-procure-titan-transtage-for-research>
6. Foster, J. E., *Impediments to Analysis: A Symposium*, Vol. 708, ASTM International, 1980.
7. Author (Anz-Meador) records; excerpt from Anon., Titan Space Launch Vehicle reference manual (actual title unknown), Sect. IV "Transtage Rocket Engine," pp. 4-6, date unknown.
8. Davis, J.G., "Development of the Titan Stage III", The Space Congress® Proceedings. Paper 4. <http://commons.erau.edu/space-congress-proceedings/proceedings-1965-2nd/session-7/4>, April 1965. Accessed 14 June 2015.
9. Davis, J. R., *Aluminum and Aluminum Alloys*, Materials Park, OH: ASM International, 1993.
10. Koleske, J. V. *Paint and coating testing manual: fourteenth edition of the Gardner-Sward handbook*. Philadelphia, PA: ASTM, 1995.
11. LIDAR Structure Sensor specs; <https://structure.io/support/what-are-the-structure-sensors-technical-specifications>. Accessed July 13, 2017
12. LIDAR Structure Sensor specs; [http://isag.jsc.nasa.gov/Content/folder1632/Handheld\\_3D\\_Scanner.htm](http://isag.jsc.nasa.gov/Content/folder1632/Handheld_3D_Scanner.htm). Accessed July 13, 2017
13. Cowardin, H., *et al.*, Observations of Titan IIIC Transtage Fragmentation Debris, AMOS 2013.
14. Lederer, S., *et al.*, "NASA's Ground-based Observing Campaigns of Rocket Bodies with the UKIRT and NASA ES-MCAT Telescopes," 7<sup>th</sup> European Conference on Space Debris, Darmstadt, Germany, April 2017.

**Annex: Titan Transtage launch history**

<i>Int. Designator</i>	<i>SSN#</i>	<i>common name</i>	<i>launch sequence</i>	<i>SLV/Tran Stage</i>	<i>launch date</i>	<i>orbit</i>	<i>Attitude control system</i>	<i>Thermal control system</i>	<i>Other</i>	
1964 081	A	949	TITAN 3A TRANSTAGE R/B	2	3A-1	10 DEC 64	LEO	biprop	P	Cb/Ti NE
1965 008	B	1000	TITAN 3A TRANSTAGE R/B	3	3A-3	11 FEB 65	LEO	biprop	P	Cb/Ti NE
1965 034	A	1359	TITAN 3A TRANSTAGE R/B	4	3A-4	06 MAY 65	LEO	biprop	P	Cb/Ti NE
1965 047	B	1413	TITAN 3C TRANSTAGE R/B	5	3C-7	18 JUN 65	LEO	biprop	P	Cb/Ti NE
1965 082	DM	1822	TITAN 3C TRANSTAGE R/B	6	3C-4	15 OCT 65	LEO	biprop	P	Cb/Ti NE
1965 108	A	1863	TITAN 3C TRANSTAGE R/B	7	3C-8	21 DEC 65	GTO	biprop	P	Cb/Ti NE
1966 053	J	2222	TITAN 3C TRANSTAGE R/B	8	3C-11	16 JUN 66	GEO	biprop	P	Cb/Ti NE
1967 003	J	2660	TITAN 3C TRANSTAGE R/B	11	3C-13	18 JAN 67	GEO	biprop	P	Cb/Ti NE
1967 040	F	2770	TITAN 3C TRANSTAGE R/B	12	3C-10	28 APR 67	HE	biprop	P	Cb/Ti NE
1967 066	G	2868	TITAN 3C TRANSTAGE R/B	13	3C-14	01 JUL 67	GEO	biprop	P	Cb/Ti NE
1968 050	J	3292	TITAN 3C TRANSTAGE R/B	14	3C-16	13 JUN 68	GEO	biprop	P	Cb/Ti NE
1968 081	E	3432	TITAN 3C TRANSTAGE R/B	15	3C-5	26 SEP 68	GEO	biprop	P	Cb/Ti NE
1969 013	B	3692	TITAN 3C TRANSTAGE R/B	16	3C-17	09 FEB 69	GEO	monoprop	HRS	Cb/Ti NE
1969 046	F	3956	TITAN 3C TRANSTAGE R/B	17	3C-15	23 MAY 69	HE	biprop	P	Cb/Ti NE
1970 027			uncataloged TranStage	18	3C-18	08 APR 70	UNK	monoprop	HRS	Cb/Ti NE
1970 093	B	4632	TITAN 3C TRANSTAGE R/B	19	3C-19	06 NOV 70	~ GEO	monoprop	HRS	Cb/Ti NE
1971 039	B	5205	TITAN 3C TRANSTAGE R/B	20	3C-20	05 MAY 71	GEO	monoprop	HRS	Cb/Ti NE
1971 095	C	5589	TITAN 3C TRANSTAGE R/B	21	3C-21	03 NOV 71	GEO	monoprop	HRS	Cb/Ti NE
1972 010	B	5854	TITAN 3C TRANSTAGE R/B	22	3C-22	01 MAR 72	GEO	monoprop	HRS	Cb/Ti NE
1973 040	B	11940	TITAN 3C TRANSTAGE R/B	23	3C-24	12 JUN 73	GEO	monoprop	HRS	Cb/Ti NE
1973 100	D	6976	TITAN 3C TRANSTAGE R/B	24	3C-26	13 DEC 73	GEO	monoprop	HRS	Cb/Ti NE
1974 039	C	7324	TITAN 3C TRANSTAGE R/B	25	3C-27	30 MAY 74	GEO	monoprop	none	Cb/Ti NE
1975 040	C	7809	TITAN 3C R/B	26	3C-25	20 MAY 75	GTO insert. Failure	monoprop	HRS	Cb/Ti NE
1975 118	C	8516	TITAN 3C TRANSTAGE R/B	27	3C-29	14 DEC 75	GEO	monoprop	none	Cb/Ti NE
1976 023	F	8751	TITAN 3C TRANSTAGE R/B	28	3C-30	15 MAR 76	GEO	monoprop	none	Cb/Ti NE
1976 059	C	8918	TITAN 3C TRANSTAGE R/B	29	3C-28	26 JUN 76	GEO	monoprop	none	Cb/Ti NE
1977 007	C	9855	TITAN 3C TRANSTAGE R/B	30	3C-23	06 FEB 77	GEO	monoprop	HRS	Cb/Ti NE
1977 034	C	10002	TITAN 3C TRANSTAGE R/B	31	3C-32	12 MAY 77	GEO	monoprop	none	Cb/Ti NE
1978 058	B	10942	TITAN 3C TRANSTAGE R/B	33	3C-33	10 JUN 78	GEO	monoprop	none	Cb/Ti NE
1978 113	D	11147	TITAN 3C TRANSTAGE R/B	34	3C-36	14 DEC 78	GEO	monoprop	none	Cb/Ti NE
1979 053	C	11436	TITAN 3C TRANSTAGE R/B	35	3C-31	10 JUN 79	GEO	monoprop	none	Cb/Ti NE
1979 086	C	11560	TITAN 3C TRANSTAGE R/B	36	3C-34	01 OCT 79	GEO	monoprop	none	Cb/Ti NE
1979 098	C	11623	TITAN 3C TRANSTAGE R/B	37	3C-37	21 NOV 79	GEO	monoprop	none	Cb/Ti NE
1981 025	C	12371	TITAN 3C TRANSTAGE R/B	38	3C-40	16 MAR 81	GEO	monoprop	none	Cb/Ti NE
1981 107	C	12932	TITAN 3C TRANSTAGE R/B	39	3C-39	31 OCT 81	GEO	monoprop	none	ITIP/Cb NE
1982 019	B	13089	TITAN 3C R/B	40	3C-38	06 MAR 82	GEO	monoprop	none	ITIP/Cb NE
1984 009	C	14677	TITAN 34D R/B(2)	41	34D-T/S-1	31 JAN 84	GEO	monoprop	none	ITIP/Cb NE
1984 037			TITAN 34D (see NOTE 1)	42	34D-T/S-2	14 APR 84	UNK	monoprop	none	ITIP/Cb NE
1984 129	B	15454	TITAN 34D R/B(2)	43	34D-T/S-3	22 DEC 84	GEO	monoprop	none	ITIP/Cb NE
1987 097	B	18584	TITAN 34D R/B	44	34D-T/S-4	29 NOV 87	GEO	monoprop	none	ITIP/Cb NE
1988 077	C	19490	TITAN 34D TRANSTAGE	45	34D-T/S-5	02 SEP 88	GEO	monoprop	none	ITIP/Cb NE
1989 035	C	19983	TITAN 34D R/B(2)	46	34D-T/S-6	10 MAY 89	GEO	monoprop	none	ITIP/Cb NE
1989 069			TITAN 34D (see NOTE 2)	47	34D-T/S-7	04 SEP 89	GEO	monoprop	none	ITIP/Cb NE

Description: **Yellow** highlighted cells indicate known Titan Transtage fragmentations. Thermal control systems are passive (P), active Heat Rejection System (HRS), or later deleted when not required to manage stage electronics (none). Other refers to engine specific status, particularly the Nozzle Extension (NE, the engine bell). The acronym ITIP indicates the Improved Transtage Injector Program while components are identified as being Columbiu (Cb; Niobium, Nb) or Titanium (Ti). Annotation UNK indicates Unknown.

Note 1: The publicly available Satellite Catalog (SatCat) identifies this launch as a Titan 34D-Agena D upper stage stack; payload OPS 7641.

Note 2: the SatCat identifies this launch as Titan 34D-Interim/Inertial Upper Stage (IUS) stack; payloads USA 43/44.